The Experimental Study of Acoustic Wave Characteristics Depends on The Load Conditions To Convert Internal Combustion Engine Outboard Motor Into Electric Outboard Motor

Endra Dwi Purnomo
Research Center for Process and Manufacturing Industry Technology, National Research and Innovation Agency of Republic Indonesia

Dewi Rianti Mandasari
Research Center for Process and Manufacturing Industry Technology, National Research and Innovation Agency of Republic Indonesia

Cuk Supriyadi Ali Nandar
Research Center for Energy Conversion and Conservation, National Research and Innovation Agency of Republic Indonesia

Aziz, Amiruddin
Research Center for Process and Manufacturing Industry Technology, National Research and Innovation Agency of Republic Indonesia

他

https://doi.org/10.5109/7236918

出版情報：Evergreen. 11 (3), pp.2791-2799, 2024-09. 九州大学グリーンテクノロジー研究教育センター
バージョン：

The Experimental Study of Acoustic Wave Characteristics Depends on The Load Conditions To Convert Internal Combustion Engine Outboard Motor Into Electric Outboard Motor

Endra Dwi Purnomo[1,*], Dewi Rianti Mandasari[1], Cuk Supriyadi Ali Nandar[2], Amiruddin Aziz[1], Lia Amelia[1], Fandy Septyan Nurgroho[1], Achmad Ridho Mubarak[1], Faisal[1]

[1]Research Center for Process and Manufacturing Industry Technology,
National Research and Innovation Agency of Republic Indonesia, DKI Jakarta, Indonesia.
[2]Research Center for Energy Conversion and Conservation,
National Research and Innovation Agency of Republic Indonesia, DKI Jakarta, Indonesia

*Author to whom correspondence should be addressed:
E-mail: endr008@brin.go.id

(Received May 13, 2024: Revised July 2, 2024: Accepted August 19, 2024).

Abstract: The maritime industry is actively transitioning to electric watercraft to curb greenhouse gas emissions and reduce dependence on fossil fuels. The Boat Motor Conversion Program, shifting from Internal Combustion Engines (ICE) to electric motors, provides an eco-friendly alternative for water transportation, addressing water pollution and noise concerns. The study focuses on the propulsion engine, utilizing a Brushless Direct Current (BLDC) motor as a boat mover. BLDC motors inherently exhibit cogging torque due to permanent magnets in the rotor interacting with the stator slots and skew angle. This article investigates the acoustic characteristics of BLDC motors, analyzing noise generated during two conditions: the motor submerged in a water tank and installed outside. Sound level data was analyzed using the Fast Fourier Transform (FFT) method to determine sound pressure values across frequencies. Results consistently show higher sound power signals for motors tested within the water tank, with Root Mean Square (RMS) differences ranging from 0.58 to 3.54 dB. Despite variations, noise levels with the motor loaded onto the outboard motor submerged in the water tank remained within acceptable limits. The findings suggest that the BLDC motor with stator skewing offers a viable solution for electric watercraft propulsion with manageable noise levels in diverse conditions.

Keywords: power spectral density; sound pressure level; noise; outboard motor

1. Introduction

In the waterways sector, electric propulsion is one of the alternative technologies to be substituted for ICE[1)]. By converting to electric motors, boats can significantly reduce their carbon footprint and minimize harmful emissions contributing to air pollution[2,3)] and global warming[4)]. However, noise pollution is an important aspect to consider in various industries, including automotive[5)], manufacturing[6,7)], and electrical equipment[8)]. The sound pressure level of electric motors can have significant implications for worker safety and environmental noise pollution[9,10)]. However, the noise requirement level for the use of noise-sensitive electric motors is no higher than for the use of electric motors for industrial applications[11,12)]. Electric motors produce high noise[13,14)], with some reaching up to 160 dBA. These noise levels can exceed the legal limits set by regulatory agencies, such as OSHA and ISO[15)]. Research efforts have revealed that the cooling fan is a major noise source in electric motors, especially those equipped with high-speed motors[16)]. Various studies have identified different sources of noise in electric motors[17,18)]. Motor noise and vibration are influenced by factors including resonance of magnetic force frequencies, natural frequencies of the stator and housing[19)], and harmonics from the supply current[20)]. Ballo et al. analyze the noise of Permanent Magnet Synchronous Electric Motors by determining the Sound Pressure Level (SPL)[21)]. Cho et al. investigate noise and vibration sources in small DC motors through visualizations and measurements, accurately identifying sources across diverse frequencies[21,22)]. Wu et al.

investigate the aerodynamic noise of the motor, primarily linked to airflow in the motor ventilation pipe and encompassing disciplines such as aerodynamics and fluid mechanics[23]. Callegaro et al. explore stator frame acoustic noise generation linked to vibration mode excitation near the stator's natural frequency, proposing a method to shape phase radial force through harmonic content analysis[24].

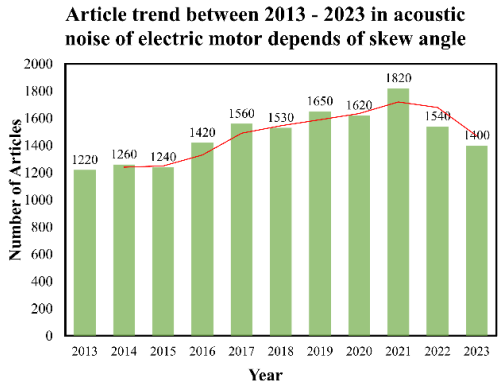

Fig. 1: Research Trend of Noise Investigation of BLDC Motor

Researchers are increasingly enthusiastic about researching and analyzing the noise of electric motors depending on the skew angle. In searching for articles on the article search engine static with the keywords "acoustic noise of electric motor depends of skew angle," found published articles that are increasing from 2013 to 2021. In this study, google scholar was used to search research articles and found the number of articles on the acoustic noise of electric motors depending on skew angle is provided in Fig. 1. 1820 articles published in 2021 were the highest number, up 46% compared to 2015. The Figure 1. also illustrates that researchers are increasingly interested in this area.

This research is a progression of the previous studies on the design of BLDC boat thruster motors[25,26] skewing stator angle with a skew angle ranging from 6º to 15º degrees shows the lowest noise is 6º degree skew. Skewing the stator of a BLDC motor has been found to reduce audible noise levels significantly[27,28]. The other research comparing electric boats (EB) and combustion engine boats (CEB) in terms of underwater radiated noise (URN), demonstrated that at a constant speed of 6 knots, the CEB exhibits higher noise levels across all frequencies. Notably, a local minimum in the EB spectrum (300–500 Hz) aligns with a local maximum in the CEB spectrum, and the CEB's tonal components are concentrated at lower frequencies due to rotating mechanical components[29]. Peak frequencies in the spectrum of sound pressure levels can additionally be associated with the characteristics of the modal motor structure and the source of excitation[30,31]. The research objective to be discussed is to investigate the noise level of the electric motor under loading conditions (propeller submerged in water) and no-load conditions. Under loading conditions, the outboard motor is mounted in the water tank, and the propeller is rotated in the water. The no-load condition occurs when the outboard motor is mounted outside the water tank and the propeller rotates outside the water. According to the International Organization for Standardization (ISO), hearing impairment is classified into categories: normal (0 – 25 dB), mild hearing loss (26 – 40 dB), moderate hearing loss (41 – 60 dB), severe hearing loss (61 – 90 dB), and profound hearing loss (>90 dB)[32]. This study confirms that previous research found electric motors with a 6-degree skew to achieve optimal noise reduction. Consequently, motors with this 6-degree skew have been experimentally tested to determine their sound spectrum characteristics both inside and outside the water tank and validate that the electric motor's noise level is lower than that of the internal combustion engine.

2. Methods

The outboard motor is equipment to drive the boat, installed in the boat's outer back. It is an independent propulsion system from the boat that can be dismantled. In this research, the internal combustion engine, which is used as the drive engine of the outboard motor, is converted to the electric motor. This study focuses on measuring the noise generated by the electric motor in the outboard motor, providing insights into its acoustic characteristics compared to the conventional internal combustion engine.

This research methodology consists of three steps: data acquisition, signal processing, and coherence analysis, as shown in Fig. 2 (a). Data acquisition for experiments was conducted under two distinct conditions to investigate the acoustic characteristics of BLDC motors under two different conditions: the motor submerged inside a water tank and the motor installed outside the water tank. The noise was recorded in a controlled chamber to minimize interference from external sources. In both conditions, the outboard motor was positioned with its propeller immersed in water at a constant depth, ensuring a steady state with no artificial waves. Sound level data were collected using a calibrated microphone placed at a radius of approximately 1 meter from the motor, per the ISO 1680 test standard. The sound levels were recorded at different motor speeds, 500 to 6000 revolutions per minute (rpm), representing typical operating conditions for electric watercraft, encompassing the lowest and highest rotations achievable by the electric motor. The electric motor experiences a high torque load at its lowest rotation, and cogging torque manifests at this minimum rotation[31]. Furthermore, there is a potential for noise generation at its highest rotation. In this study, the noise of the electric motor is recorded at every increment of 500 rpm.

This experiment setup, illustrated in Fig. 2 (b) and (c), ensured consistent measurements of the motor's acoustic performance in different environments. The specifications

for the outboard motor and test equipment can be observed in Table 1.

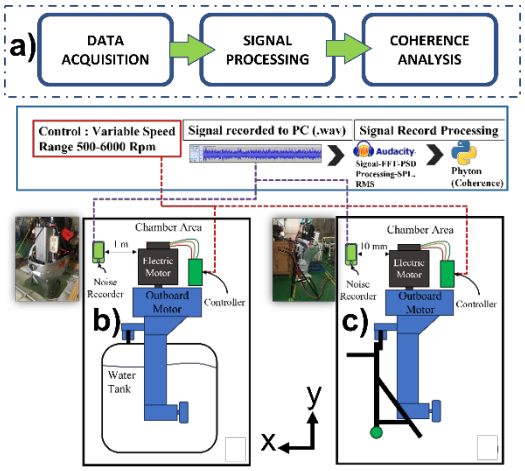

Fig. 2. (a) Reseach Method; Experimental Setup: (b) Outboard Motor Installed in The Water Tank; (c) Outboard Motor Installed Outside Water Tank

Table 1. Outboard Motor and Equipment Specifications.

Parameter	Value	Unit
Motor type	BLDC IPM V-Shape	-
Input voltage	72	VDC
Number of Phases	3	-
Number of Slots	12	-
Number of Pole	8	-
Motor diameter	230	mm
Motor length	290.5	mm
Stator outer diameter	175	mm
Rotor outer diameter	98.8	mm
Lamination length	105	mm
Skew stator	10	°
Magnet thickness	3	mm
Magnet width	14.3	mm
Chamber	3	m^3
Tank Capacity	1000	lt
Water Volume	851	lt
Length of Submerged Propeller	50	mm
Microphone	1	-
Radius of Recording	1	m
Sensitivity	-3	dB
Test Condition	**Ambient Temp**	
Water	27	°C
Air	30	°C
Motor Casing	33	°C
Components	**Materials**	
Motor	Alumunium Alloy	
Prop	Stainless Steel	
Water Tank	HDPE	
Chamber	3D GOM, Foam, Rubber	

After the noise recording, the data was processed using the FFT method to convert time-domain signals into the frequency domain. This conversion was performed using Audacity, an open-source tool for signal processing. Audacity supports various sample rates, and research has demonstrated its effectiveness in recording noise levels of loudspeakers[31]. Higher sample rates provide better accuracy in recording high frequencies, making Audacity suitable for this study. The transformed data were then analyzed to obtain Power Spectral Density (PSD) and RMS values representing the average sound level. The use of Audacity ensured precise and reliable conversion and analysis of the acoustic data, facilitating a detailed examination of the motor's noise characteristics.

Understanding the relationship between noise levels at different motor speeds involved performing a coherence analysis. The coherence function quantifies the similarity between two signals in the frequency domain, offering insights into how noise characteristics change with speed. Sound pressure levels were converted and analyzed based on the assumption that the measurement of field conditions can be expressed in equation (1), where SPL is the sound power level (dB), $SPLa$ is the average of the sound pressure level (dB), and r is the theoretical radius of the measurement boundary (m).

$$SPL = SPLa + 10\,Logr + 0.5dB \tag{1}$$

Coherence expresses a relationship indicating how the x signal is attached to the y signal identically. A coherence magnitude close to zero means no influence, and close to 1 has a strong impact. In complex terms, coherence can be expressed in equation (2).

$$C_{xy}(f) = \frac{\widehat{|S_{xy}(f)|^2}}{\sqrt{\hat{S}_{xy}(f)\hat{S}_{yy}(f)}} \tag{2}$$

Where the value $\hat{S}_{xx}(f)$ is PSD of the signal x, then $\hat{S}_{yy}(f)$ is PSD of signal y, the value of $\hat{S}_{xy}(f)$ is the cross-spectral density of x and y. It can be stated that the resonant frequency is shown by the peak, as indicated by the high coherence value[32].

The coherence analysis was conducted with three-speed comparisons under two conditions: inside and outside the water tank. The specific speed comparisons were 1000 rpm and 3000 rpm; 1000 rpm and 6000 rpm; and 3000 rpm and 6000 rpm. For each speed pair, coherence analysis quantified the similarity between the noise signals at the respective speeds in the submerged (inside water tank) and non-submerged (outside water tank) conditions. This approach provided detailed insights into the acoustic performance of the BLDC motor, highlighting how different operating environments and motor speeds influence noise behavior. Peaks in the coherence function indicated resonant frequencies, with high coherence values suggesting strong relationships between the noise signals at different speeds. The results were plotted on a semilogarithmic scale using Python. The Python code for coherence analysis is shown in Fig. 3, which compares the data at 1000 rpm and 3000 rpm inside the water tank.

```
AdanB = np.abs(decibel_3000_on / decibel_1000_on)
Pedoman = np.ones_like(frequency)

result_df = pd.DataFrame({'Frequency': frequency, 'Coherence_1000_vs_3000': AdanB})
result_file_path = os.path.join(output_folder, 'coherence_1000 vs 3000_semilog.csv')
result_df.to_csv(result_file_path, index=False)

plt.semilogx(frequency, AdanB, label='Coherence 3000 RPM / 1000 RPM')
plt.plot(frequency, Pedoman, label='Pedoman y=1', linestyle='--')
plt.title('Coherence between 1000 RPM and 3000 RPM Signals')
plt.xlabel('Frequency (Hz)')
plt.ylabel('Coherence')
plt.legend(bbox_to_anchor=(1.05, 1), loc='upper left', borderaxespad=0.)

plt.grid(True)
plt.show()
```

Fig. 3: Coherence Analysis Between 1000 rpm and 3000 rpm Inside the Water Tank using Python

3. Results

The level of airborne sound power emitted by the motor is greatly affected by the structure and environmental conditions. Each motor shaft and propeller compartment structure generates noise and transfers vibration energy between motor structures. During the testing process, the vibration source of the jig must be minimized because the sound source is captured through the air. Visually, the waveform track of Fig. 4a. tested under load is more dominated by random signals than Fig. 4b. with no load. From the results of the signal recording track in both conditions, the power spectral density value of each condition was investigated.

Spectrum plots are plotted as a logarithmic scale, as shown in Fig. 5. to Fig. 10. The FFT analysis provides the data and determines the number of bins based on the FFT size. Since no DC bin is added for 1024, it will produce 511 frequency bins. The digital maximum is 0 dB, which stands for zero decibels full scale. Consequently, digital decibel level readings are typically negative (-dB). In integer formats, 0 dB is the highest value obtained within a specific bit depth, even if 24-bit audio files have more digits than 8-bit ones. Thus, as the default, an 8-bit file at 0 dB sounds no louder than a 24-bit file at 0 dB.

Figure 5, Figure 6, and Figure 7 show that the random excitation rises with increasing motor speed, depending on the excitation position on the outboard motor testing platform in the water tank. The primary source of propeller noise is cavitation induced by the propeller rotation[33], creating areas of low pressure at the blade tip and surface, leading to the formation and rapid collapse of numerous air bubbles, resulting in robust and impulsive noise. The results indicate that when the electric boat's rotation speed rises, it consequently increases the noise intensity and spectrum height. Furthermore, a spectrum level indicates the noise level, with peaks significantly influencing the overall sound pressure level (OASPL)[34]. One hertz (Hz) is added to the estimated frequency, which falls between 30 and 30000 Hz. In this frequency range, random noise fluctuations occur. Then, the frequency range of 300 Hz randomly begins to experience a decrease in sound power level (dB).

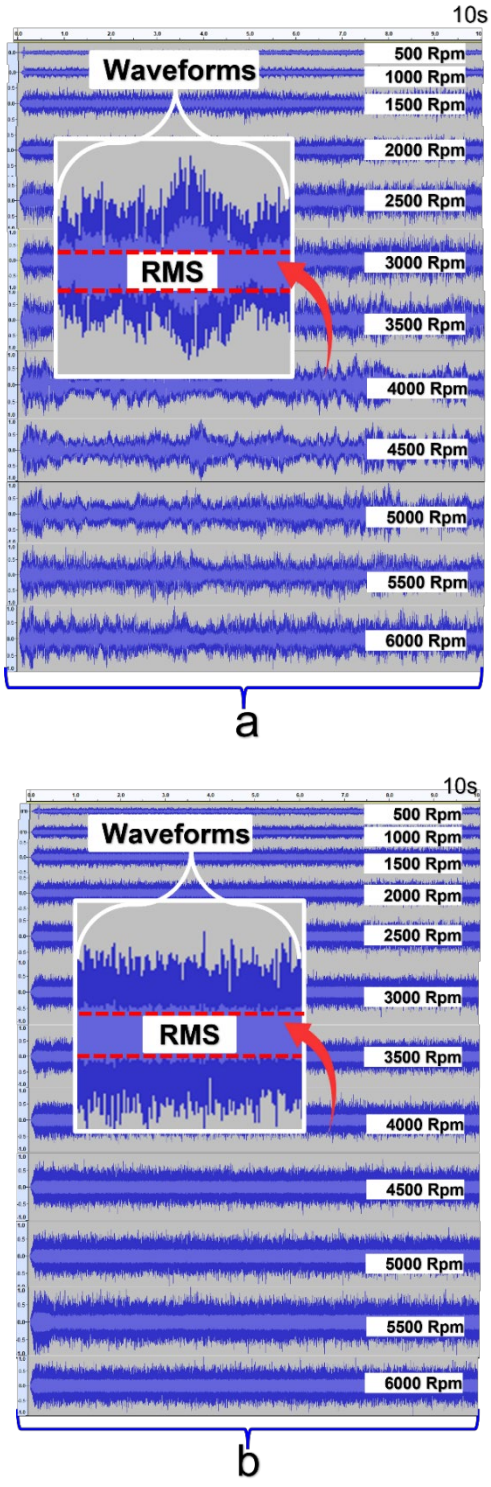

Fig. 4: Signal Noise Recorded (a)Motor Inside Water Tank (b) Outside Water Tank

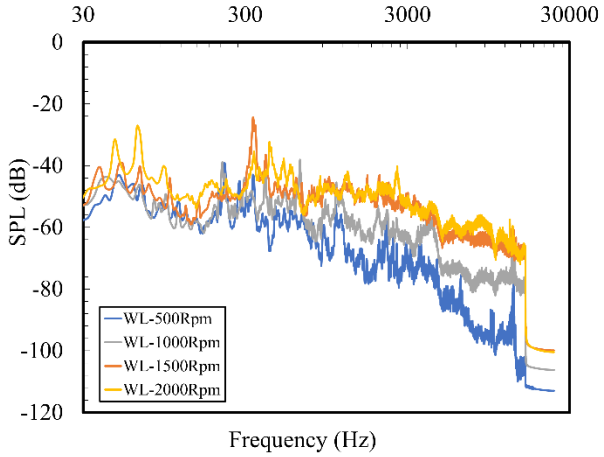

Fig. 5: PSD Outboard Installed Inside Water Tank 500-2000 rpm

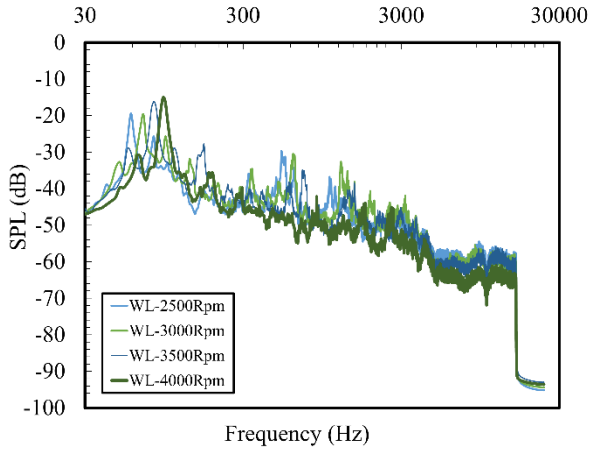

Fig. 6: PSD Outboard Installed Inside Water Tank 2500-4000 rpm

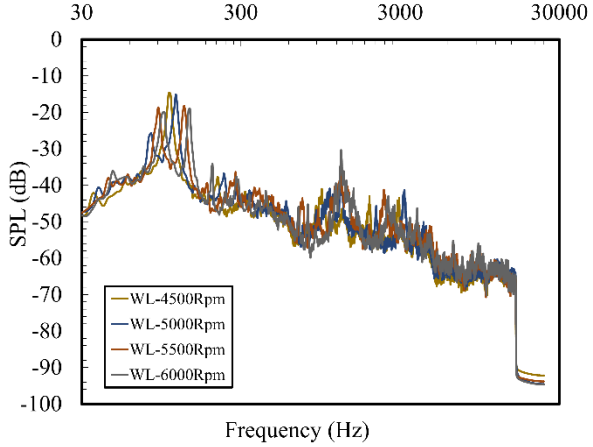

Fig. 7: PSD Outboard Installed Inside Water Tank 4500-6000 rpm

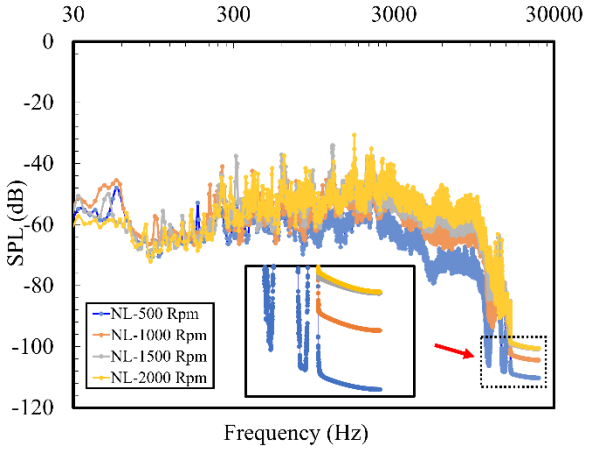

Fig. 8: PSD Outboard Installed Inside Water Tank 500-2000 rpm

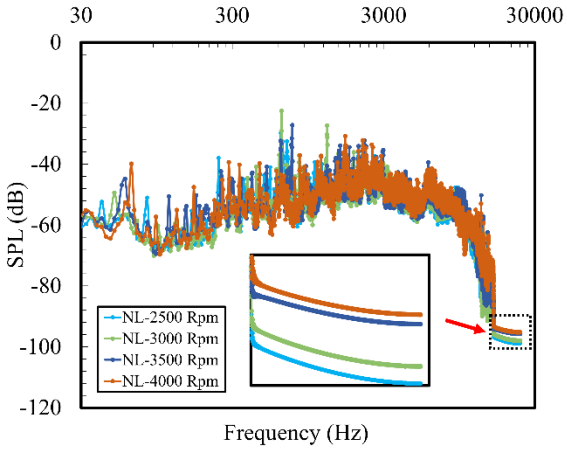

Fig. 9: PSD Outboard Installed Inside Water Tank 2500-4000 rpm

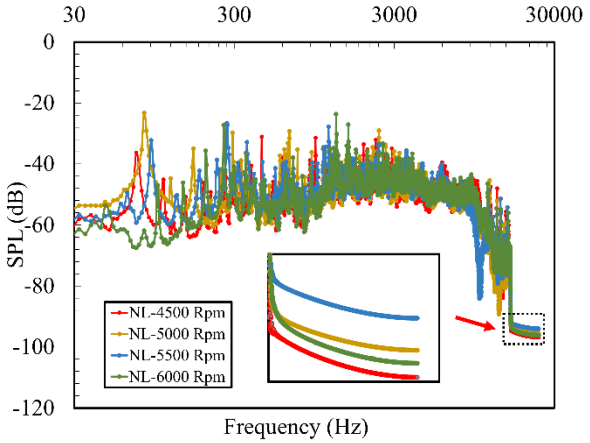

Fig. 10: PSD Outboard Installed Inside Water Tank 4500-6000 rpm

The peak noise level of the electric boat motor test outside the water tank, as shown in Fig. 8, Fig. 9, and Fig. 10, is inside the water tank testing. The no-load test had lower noise variability with each increase in motor speed than the water test.

The RMS curve is shown in Fig. 11. From the speed of 500 rpm, the SPL (dB) value curve rises until 1500 rpm but at 1500 rpm the noise drops randomly until 2000 rpm increases.

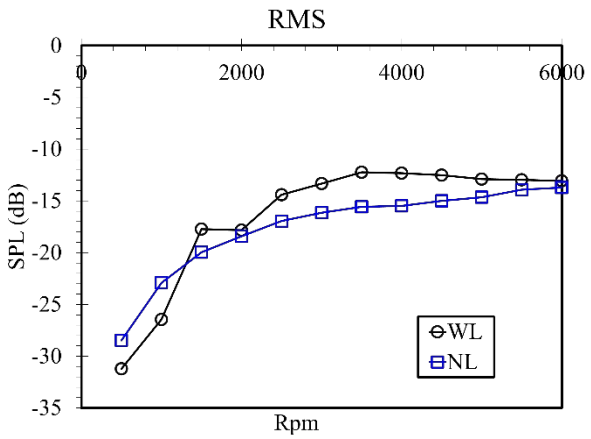

Fig. 11: RMS of outboard test inside and outside water tank

The purpose of the coherence analysis function is to indicate the linear relationship between the motor rotation signals and their comparison[35]. It has been partially applied to determine the overall response to vibroacoustic electric motorboat structures.[36] Figure 12 presents the coherence between the signals at 1000 rpm and 3000 rpm inside water tank testing. The average coherence value is around 0.82, indicating that between these two signals, it is likely that the peak is the resonant frequency. The coherence of the 1000 and 6000 rpm signals in Figure 13 and Figure 14 indicates an average coherence value of 0.85 and close to 1, respectively, so the confidence level is high that the peak is a resonant frequency.

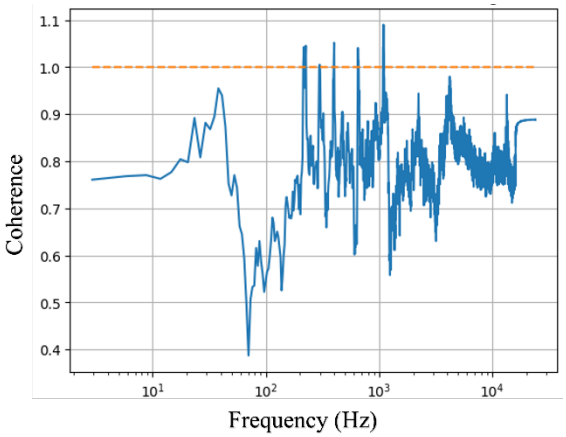

Fig. 12: Coherence Between Signal 1000 rpm and 3000 rpm Inside Water Tank

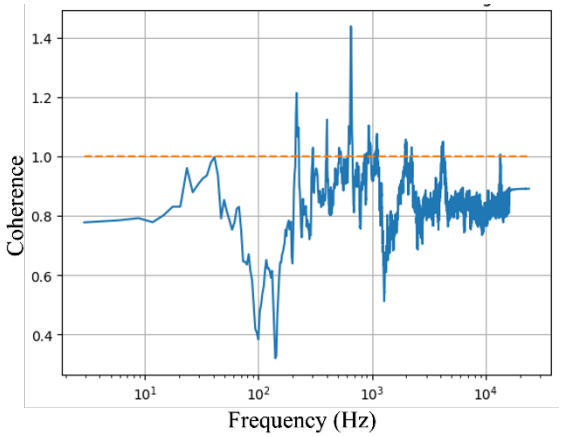

Fig. 13: Coherence Between Signal 1000 rpm and 6000 rpm Inside Water Tank

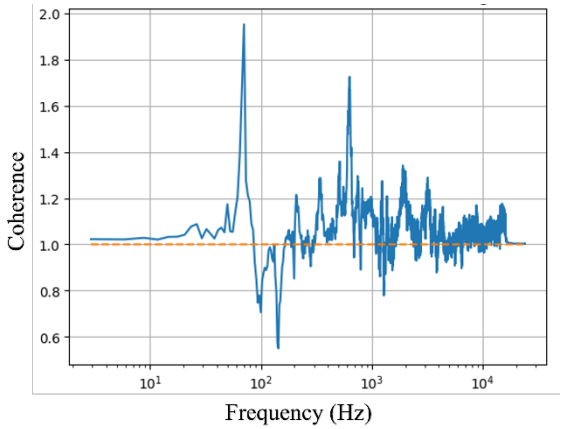

Fig. 14: Coherence Between Signal 3000 rpm and 6000 rpm Inside Water Tank

The interpretation and delineation of boundaries for the coherence function are rendered challenging by the substantial influence of noise and the multi-signal interference effect. The measurement of signal amplification can be undertaken utilizing an estimated coherence length characterized by a coefficient of variation[37].

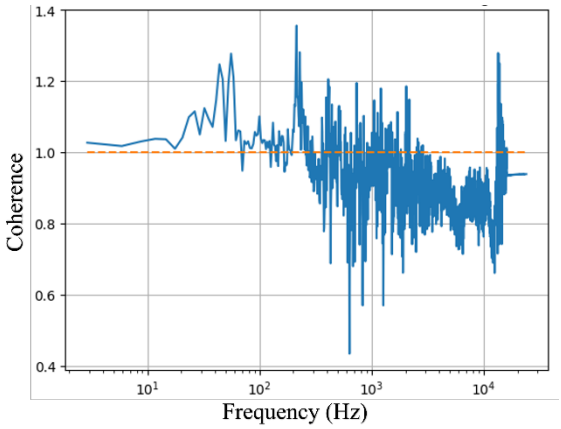

Fig. 15: Coherence Between Signal 1000 rpm and 3000 rpm Outside Water Tank

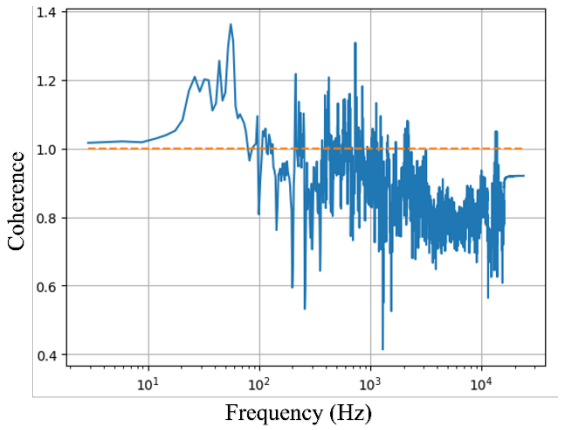

Fig. 16: Coherence Between Signal 1000 rpm and 6000 rpm Outside Water Tank

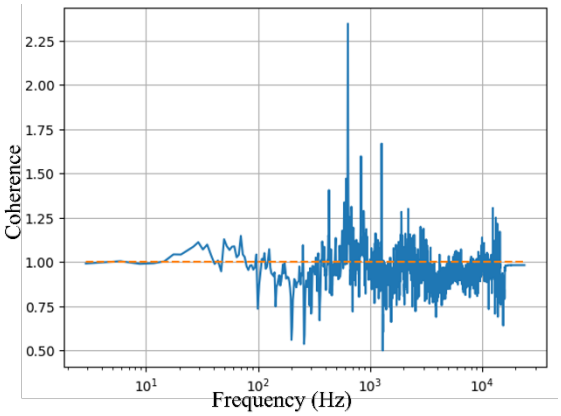

Fig. 17: Coherence Between Signal 3000 rpm and 6000 rpm Outside Water Tank

The coherence values of the testing signals outside the water tank are depicted in Fig. 15, Fig. 16, and Fig. 17. The coherence value of the noise signal at 1000 rpm, compared to 3000 rpm, is 0.90, as indicated in Fig. 15. This value suggests a high-reliability level, representing the resonance peak. Similarly, the coherence values for rotational speed at 1000 rpm compared to 6000 rpm as indicated in Fig. 16 and 3000 rpm compared to 6000 rpm as indicated in Fig. 17 are 0.85 and 0.94, respectively. Consequently, the overall confidence level in its resonance peak is high under this unloaded testing condition.

As a comparison, a previous study conducted on the use of combustion engines for boats showed underwater radiated noise test values with variations in 3-speed modes at 6 knots or equivalent to 2000 rpm in the frequency range of 102 Hz to 103 Hz, with the highest SPL reaching up to 140 dB[38]. Compared to the tests in this current study, the SPL values at 2000 rpm for underwater immersion testing were less than 120 dB. The underwater noise of submerged electric motors tends to be lower than electric boats with internal combustion engines.

4. Conclusion

The outboard motor noise levels tested within the water tank exhibit a consistently higher average sound power signal than those tested outside the tank. It can be asserted that the RMS value serves as a benchmark for comparing the average noise levels under the two testing conditions. The RMS difference between the testing of the electric motor propelled within the water tank ranges from 0.58 dB to 3.54 dB. The highest RMS value for the water-loaded motor occurs at 3000 rpm, registering at -12.23 dB, whereas for the unloaded condition, the highest RMS value at 6000 rpm is -13.37 dB. Compared to a previous study that reported underwater radiated noise levels of up to 140 dB at 2000 rpm for combustion engines, the current study reveals that submerged electric motors produce significantly lower SPL values, below 120 dB, indicating quieter operation.

Acknowledgment

The research supports the Indonesian Maritime Government's program to develop a sustainable electric boat motor pilot project for coastal areas in Indonesia. BRIN collaborates with partners such as PT GEMPACS Ltd, PT OCTAGON, and PT NICE Indonesia.

Nomenclature

$\hat{S}_{xx}(f)$	Power Spectral Density (PSD)
$SPLa$	Average Sound Pressure Level (dB)
SPL	Sound Power Level (SPL)
$\hat{S}_{xy}(f)$	Cross-Spectral Density (CSD)
$C_{xy}(f)$	Coherence
RMS	Root Mean Square

References

1) J.E. Candelo-Beccera, L.B. Maldonado, E.P. Sanabria, H.V. Pestana, and J.J. García, "Technological alternatives for electric propulsion systems in the waterway sector," Energies (Basel), 16 (23) 7700 (2023). doi:10.3390/en16237700.
2) Lalit N. Patil, Hrishikesh P. Khairnar, J. A. Hole, D. M. Mate, A.V. Dube, R. N. Panchal, and V. B. Hiwase, "An experimental investigation of wear particles emission and noise level from smart braking system," Evergreen, 9 (3) 711–720 (2022). doi:10.5109/4843103.
3) R. Kumar, A. Kanwal, M. Asim, M. Pervez, M.A. Mujtaba, Y. Fouad, and M.A. Kalam, "Transforming the transportation sector: mitigating greenhouse gas emissions through electric vehicles (evs) and exploring sustainable pathways," AIP Adv, 14 (3) (2024). doi:10.1063/5.0193506.
4) A.C.R. Mayer, J. Mayer, M. Wyser, F. Legerer, J. Czerwinski, T.W. Lutz, T. V. Johnson, and M.Z. Jacobson, "Particulate filters for combustion engines to mitigate global warming. estimating the effects of

a highly efficient but underutilized tool," Emission Control Science and Technology, 10 (1) 10–21 (2024). doi:10.1007/s40825-023-00236-x.

5) G. Burshukova, A. Kanazhanov, R. Abuova, and A. Joldassov, "Analysis of using damping alloys to improve vibration and strength characteristics in the automotive industry," Evergreen, 10 (2) 742–751 (2023). doi:10.5109/6792824.
6) Y. Shen, and X. Zhang, "Intelligent manufacturing, green technological innovation and environmental pollution," Journal of Innovation & Knowledge, 8 (3) 100384 (2023). doi:10.1016/j.jik.2023.100384.
7) Rikhotso, Harmse, and Engelbrecht, "Noise sources and control, and exposure groups in chemical manufacturing plants," Applied Sciences, 9 (17) 3523 (2019). doi:10.3390/app9173523.
8) E. Król, M. Maciążek, and T. Wolnik, "Review of vibroacoustic analysis methods of electric vehicles motors," Energies (Basel), 16 (4) (2023). doi:10.3390/en16042041.
9) A. Habibie, M. Hisjam, W. Sutopo, and M. Nizam, "Sustainability evaluation of internal combustion engine motorcycle to electric motorcycle conversion," Evergreen, 8 (2) 469–476 (2021). doi:10.5109/4480731.
10) I. Deryabin, "On reducing the noise of the internal combustion engine of a motor vehicle," Transportation Research Procedia, 61 505–509 (2022). doi:10.1016/j.trpro.2022.01.082.
11) P. Gonzalez, G. Buigues, and A.J. Mazon, "Noise in electric motors: a comprehensive review," Energies (Basel), 16 (14) (2023). doi:10.3390/en16145311.
12) P. Gonzalez, G. Buigues, and A.J. Mazon, "Noise in electric motors: a comprehensive review," Energies (Basel), 16 (14) 5311 (2023). doi:10.3390/en16145311.
13) L.N. Patil, and H.P. Khairnar, "Investigation of human safety based on pedestrian perceptions associated to silent nature of electric vehicle," Evergreen, 8 (2) 280–289 (2021). doi:10.5109/4480704.
14) C. Stuckmann, "Noise & Vibration Levels of modern Electric Motors," in: 2016. https://api.semanticscholar.org/CorpusID:113527616.
15) O. Rikhotso, J.L. Harmse, and J.C. Engelbrecht, "Noise sources and control, and exposure groups in chemical manufacturing plants," Applied Sciences (Switzerland), 9 (17) (2019). doi:10.3390/app9173523.
16) H. Li, "Effects of edge geometry on flow driving of a stamped metal cooling fan," Engineering Applications of Computational Fluid Mechanics, 4 (4) 532–548 (2010). doi:10.1080/19942060.2010.11015339.
17) R. Wang, T. Liu, C. Zhang, L. Yu, and J. Li, "Noise source localization in permanent magnet synchronous motors under time-varying speed working conditions," Applied Acoustics, 192 108724 (2022). doi:10.1016/j.apacoust.2022.108724.
18) D. Hu, P. Xu, C. Cao, X. Yan, Z. Hu, Z. Song, and H. Li, "Experimental research on the sound recognition of the electric vehicle motor," MATEC Web of Conferences, 309 03033 (2020). doi:10.1051/matecconf/202030903033.
19) S. Čorović, and D. Miljavec, "Modal analysis and rotor-dynamics of an interior permanent magnet synchronous motor: an experimental and theoretical study," Applied Sciences, 10 (17) 5881 (2020). doi:10.3390/app10175881.
20) E. Król, and M. Maciążek, "Identification and analysis of noise sources of permanent magnet synchronous traction motor with interior permanent magnet," Energies (Basel), 16 (16) (2023). doi:10.3390/en16166018.
21) F. Ballo, M. Gobbi, G. Mastinu, and R. Palazzetti, "Noise and vibration of permanent magnet synchronous electric motors: a simplified analytical model," IEEE Transactions on Transportation Electrification, 9 (2) 2486–2496 (2023). doi:10.1109/TTE.2022.3209917.
22) Y.T. Cho, "Characterizing sources of small dc motor noise and vibration," Micromachines (Basel), 9 (2) (2018). doi:10.3390/mi9020084.
23) B. Wu, and M. Qiao, "A review of the research progress of motor vibration and noise," International Transactions on Electrical Energy Systems, 2022 5897198 (2022). doi:10.1155/2022/5897198.
24) A.D. Callegaro, B. Bilgin, and A. Emadi, "Radial force shaping for acoustic noise reduction in switched reluctance machines," IEEE Trans Power Electron, 34 (10) (2019). doi:10.1109/TPEL.2019.2891050.
25) D.R. Mandasari, K. Yulianto, L. Amelia, A. Aziz, E. Dwi Purnomo, Faisal, and C.S.A. Nandar, "Design and optimization of brushless dc motor for electric boat thruster," Evergreen, 10 (3) 1928–1937 (2023). doi:10.5109/7151773.
26) R. Dewi Mandasari, L. Amelia, A. Iman Malakani, E. Dwi Purnomo, A. Aziz, A. Andi Suryandi, A. Krisnowo, and C. Supriyadi Ali Nandar, "Reduction of cogging torque in segmented permanent magnet bldc motor ipm v-shape by skewing stator," AIP Conf Proc, 2932 (1) (2023). doi:https://doi.org/10.1063/5.0174906.
27) Z. Shi, X. Sun, Y. Cai, Z. Yang, G. Lei, Y. Guo, and J. Zhu, "Torque analysis and dynamic performance improvement of a pmsm for evs by skew angle optimization," IEEE Transactions on Applied Superconductivity, 29 (2) 1–5 (2019). doi:10.1109/TASC.2018.2882419.
28) M. Jagiela, E.A. Mendrela, and P. Gottipati, "Investigation on a choice of stator slot skew angle in brushless pm machines," Electrical Engineering, 95 (3) 209–219 (2013). doi:10.1007/s00202-012-0252-8.
29) H.J. Lee, S.U. Chung, and S.M. Hwang, "Noise

source identification of a bldc motor," Journal of Mechanical Science and Technology, 22 (4) 708–713 (2008). doi:10.1007/s12206-008-0110-9.
30) S. Hu, S. Zuo, M. Liu, H. Wu, and Z. Liu, "Modeling and analysis of radial electromagnetic force and vibroacoustic behaviour in switched reluctance motors," Mech Syst Signal Process, 142 106778 (2020). doi:10.1016/j.ymssp.2020.106778.
31) E.D. Purnomo, Ubaidillah, F. Imaduddin, I. Yahya, and S.A. Mazlan, "Preliminary experimental evaluation of a novel loudspeaker featuring magnetorheological fluid surround absorber," Indonesian Journal of Electrical Engineering and Computer Science, 17 (2) 922–928 (2019). doi:10.11591/ijeecs.v17.i2.pp922-928.
32) R. Brincker, L. Zhang, and P. Andersen, "Modal identification of output-only systems using frequency domain decomposition," Smart Mater Struct, 10 (3) 441–445 (2001). doi:10.1088/0964-1726/10/3/303.
33) Y. Su, S. Kim, and S. Kinnas, "Prediction of propeller-induced hull pressure fluctuations via a potential-based method: study of the effects of different wake alignment methods and of the rudder," J Mar Sci Eng, 6 (2) 52 (2018). doi:10.3390/jmse6020052.
34) Y. Xu, and W. Zhao, "The Study on Noise Characteristics of Underwater Electric Propulsion," in: 2021 OES China Ocean Acoustics (COA), 2021: pp. 487–490. doi:10.1109/COA50123.2021.9519861.
35) M. AKAR, S. TAŞKIN, Ş.S. ŞEKER, and İ. ÇANKAYA, "Detection of static eccentricity for permanent magnet synchronous motors using the coherence analysis," Turkish Journal of Electrical Engineering and Computer Sciences, (2010). doi:10.3906/elk-0911-298.
36) R. Fan, Z. Su, G. Meng, and C. He, "Application of sound intensity and partial coherence to identify interior noise sources on the high speed train," Mech Syst Signal Process, 46 (2) 481–493 (2014).
37) W.M. Carey, "The determination of signal coherence length based on signal coherence and gain measurements in deep and shallow water," J Acoust Soc Am, 104 (2) 831–837 (1998).
38) T. Gaggero, E. Armelloni, A. Codarin, C. Chicco, M. Spoto, C. Franzosini, S. Ciriaco, and M. Picciulin, "Electric boat underwater radiated noise and its potential impact on species of conservation interest," Mar Pollut Bull, 199 115937 (2024). doi:10.1016/j.marpolbul.2023.115937.